DOI 10.1007/s10527-020-10011-9
Biomedical Engineering, Vol. 54, No. 4, November, 2020, pp. 235-239. Translated from Meditsinskaya Tekhnika, Vol. 54, No. 4, Jul.-Aug., 2020, pp. 4-7.
Original article submitted June 17, 2020.

A Printed Antenna with an Infrared Temperature Sensor for a Medical Multichannel Microwave Radiometer

S. G. Vesnin[1,2], M. K. Sedankin[1,3], A. G. Gudkov[1]*, V. Yu. Leushin[1], I. A. Sidorov[1], I. O. Porokhov[4], S. V. Agasieva[5], and S. I. Vidyakin[1]

The results of designing a printed ultra-wideband antenna intended for use as a part of a multichannel microwave radiometer are presented. The design of a ring-shaped antenna with a built-in infrared sensor for measuring skin temperature is proposed. The results of numerical simulation of the electromagnetic field of the antenna in tissues of a biological object are presented. The results of calculating the voltage standing wave ratio, measurement depth of the antenna, the resolution, and the distribution of radiation power over the tissue volume under study are presented.

Introduction

In recent years, there has been a growing interest in medical microwave radiometry [1-11]. In contrast to infrared thermography, which allows visualizing the skin temperature, microwave radiometry provides for identification of thermal anomalies in biological tissues at a depth of 5-7 cm. In many cases, it is important to measure both the internal and the skin temperature. This makes it possible to take into account both contributions to the measured brightness temperature and thereby increase the accuracy of detecting deep thermal anomalies [11]. Antennas used in currently available commercial medical radiometers are implemented as complex waveguide systems of rather large size and weight, which hinders their use in multichannel systems. The development of ultra-wideband antennas several centimeters in size and the reduction of the overall dimensions of their radiometric receivers open up the possibility of creating a multichannel multifrequency radiometer [5] based on the positive experience in developing antennas using modern materials and advanced technologies [9, 10]. The goal of this work was to suggest a design and to model performance of a small-size ultra-wideband antenna with a built-in infrared (IR) sensor that could be used in a multichannel multifrequency radiometer for 3D imaging of the brightness temperature distribution inside a biological object.

Methods

The relationship between the brightness temperature T_{br} measured with a medical radiometer and the thermodynamic temperature $T(r)$ of human tissues is given by the following equation:

$$T_{br} = \int_{-\infty}^{\infty} T(r)W(r)dV; \quad W(r) = \frac{\frac{\sigma(r)}{2}|E(r)|^2}{\int_{-\infty}^{\infty} \frac{\sigma(r)}{2}|E(r)|^2 dV}, \quad (1)$$

where $W(r)$ is the radiometric weighting function of the antenna, $|E(r)|^2$ is the squared electric field, $\sigma(r)$ is the electrical conductivity of tissue, and r is the running coordinate. Development of the antenna should involve simulation of electromagnetic and thermal fields of bio-

[1] Bauman Moscow State Technical University, Moscow, Russia; E-mail: ooo.giperion@gmail.com
[2] RES Company, Moscow, Russia.
[3] Burnazyan Federal Medical Biophysical Center, Federal Medical Biological Agency of the Russian Federation, Moscow, Russia.
[4] Central Scientific Research Radio Engineering Institute named after Academician A.I. Berg, Moscow, Russia.
[5] Peoples' Friendship University of Russia, Moscow, Russia.
* To whom correspondence should be addressed.

TABLE 1. Parameters of Biological Tissues within the Frequency Range under Consideration [10]

Parameters	Skin	Breast tissues	Muscles	Malignant tumor
Permittivity ε	36.75	10	51.1	50
Electrical conductivity σ, S/m	2.21	0.4	2.82	2
Layer thickness, mm	2	88	10	–

logical objects [7, 9, 10, 12, 13]. The HIPERCONE FDTD software for electrodynamic simulation based on the Electromagnetic Template Library (EMTL) was used for electric field computation by numerical methods [14]. The suggested antenna design is shown in Fig. 1a. A printed ring-shaped ultra-wideband source antenna operating within a frequency band of 3.4-4.2 GHz is used. It is compatible with an IR sensor for remote measurement of skin temperature. Figure 1b shows the topology of the printed circuit board of the antenna. The board is made of 1.28-mm-thick RO3010 laminate (permittivity ε = 10.2). To meet the requirements for noise immunity, the antenna housing is implemented as a hollow metal cylinder 32 mm in diameter and 6 mm in height. The housing is open on one side. It contains the printed circuit board of the antenna and a shielded Melexis MLX90615SSG-DAA IR sensor. The estimated weight of the antenna is 8 g. A multilayer breast model was used for electric field computation (Fig. 2a). It simulates several biological tissues: skin, breast and muscle tissues, and malignant tumor. Each layer has its own electrical conductivity, permittivity, and thickness (Table 1). The dimensions of the multilayer breast model are as follows: length, 100 mm; thickness, 100 mm; height, 100 mm.

Results

Figure 2b shows the calculated frequency dependence of the voltage standing wave ratio (VSWR) of the developed antenna. The main specific feature of the antenna is a broader operating frequency band. It can be seen from Fig. 2b that the antenna VSWR in the frequency band of 2800-5200 MHz is less than 1.5; i.e., the operating frequency bandwidth is 2400 MHz, which considerably exceeds that of the antennas used in the commercially available devices [15]. This makes it possible to use the same antenna in several frequency ranges of operation of multichannel multifrequency radiometers with 3D visualization of the internal brightness temperature distribution.

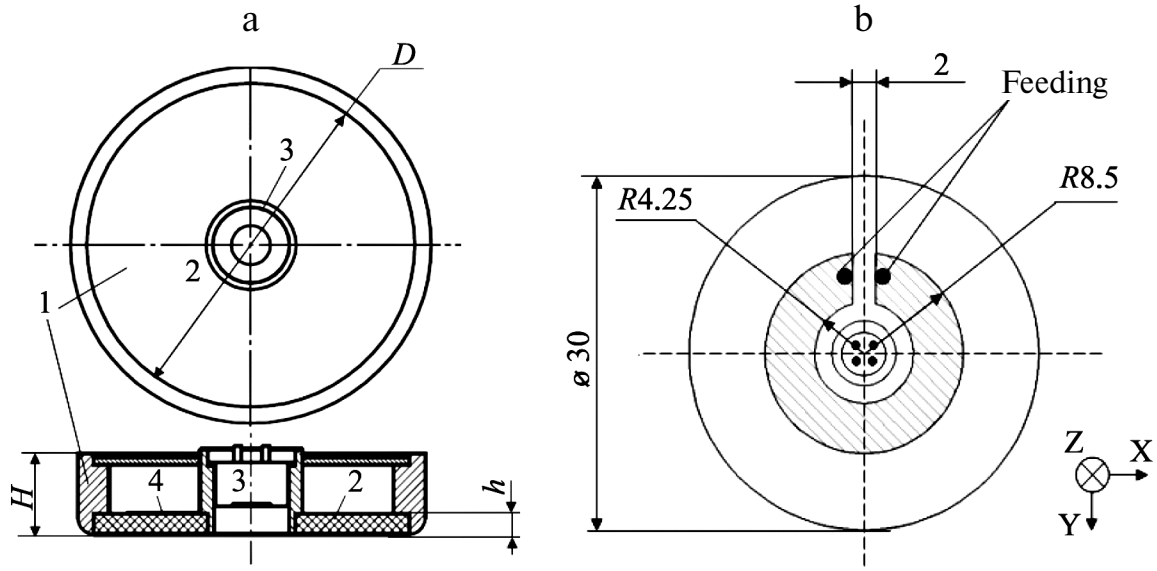

Fig. 1. Design of the broadband antenna with a built-in IR sensor. a) Structure of the antenna: 1 – shielding housing; 2 – substrate; 3 – IR sensor; 4 – source antenna; b) topology of the printed circuit board of the antenna.

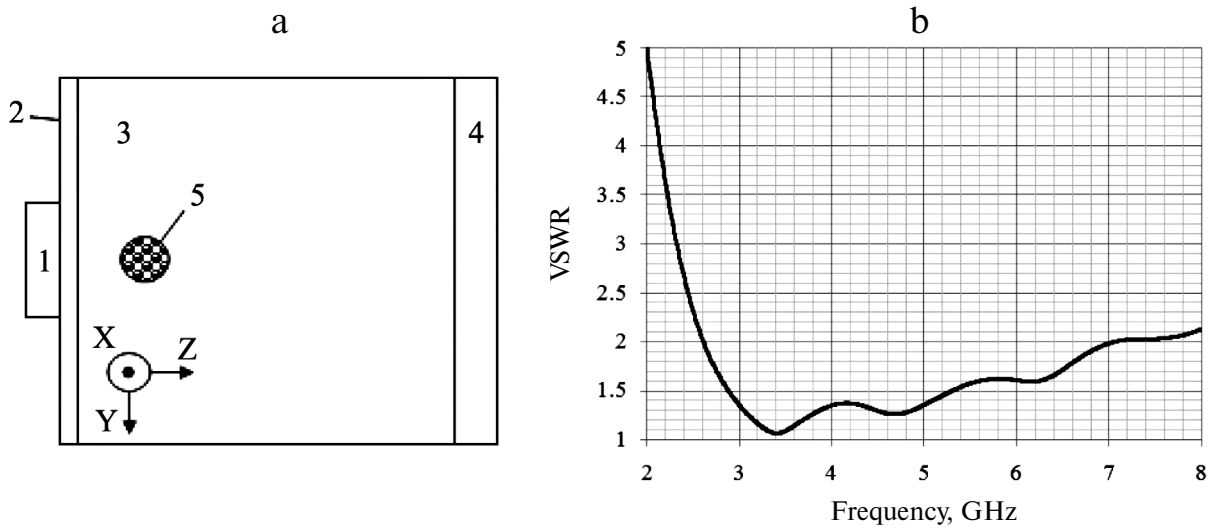

Fig. 2. Computational model of a biological object and results of VSWR calculation. a) Multilayer model: 1 – antenna; 2 – skin; 3 – breast tissue; 4 – muscles; 5 – tumor; b) antenna VSWR vs. frequency curve.

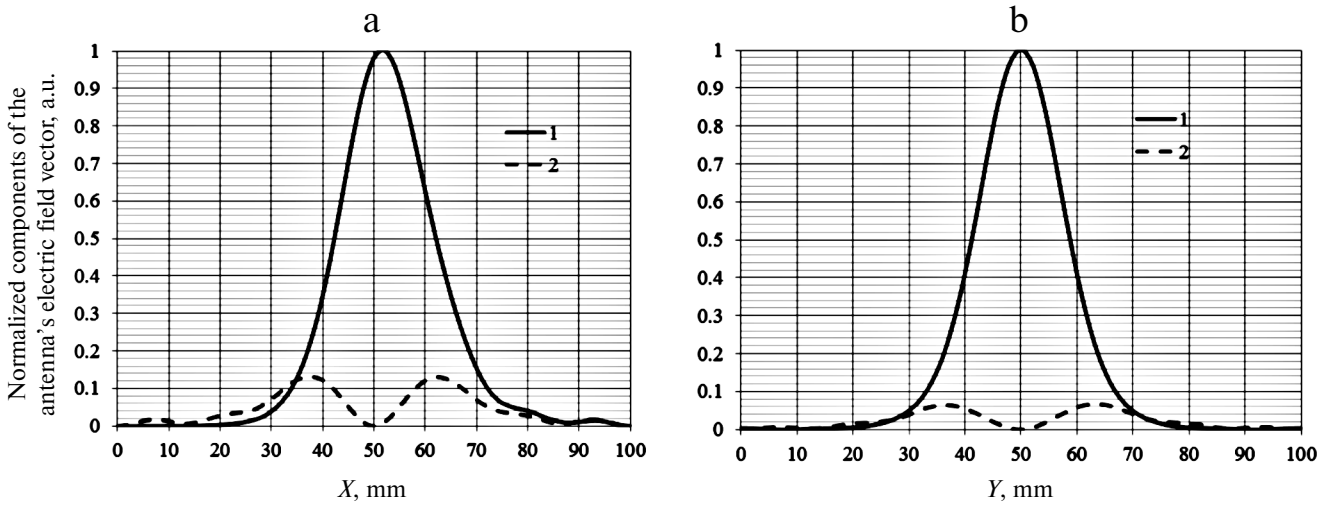

Fig. 3. Normalized components of the antenna's electric field vector at a depth of 20 mm in the E-plane (a) and the H-plane (b): 1 – E_x^2; 2 – E_z^2.

Figure 3 shows the calculated distributions of the normalized components of the antenna's electric field vector at a depth of 20 mm in the E-plane (a) and the H-plane (b). It can be seen that there is a noticeable predominance of the X-component of the electric field, while E_y is close to zero.

When describing fields in the near-field region, the conventional parameters used to describe antennas in the far-field region (radiation pattern, gain, etc.) cannot be applied. For this reason, we have developed and used a system of parameters allowing different antennas to be compared. The depth of measurement of the brightness temperature provided by a microwave radiometer is usually defined as the depth of plane wave penetration into biological tissues. At 3.8 GHz, this depth for the breast tissue is 42 mm. However, the electric field of the antenna is different from a plane wave, so that the measurement depth is also different. For this reason, it was proposed to calculate the volume in which 85% of the power radiated by the antenna is dissipated to find the depth of

TABLE 2. Comparison of Parameters of Printed and Waveguide Antennas

	F_0, GHz	ΔF, MHz	D, mm	W_z, mm	W_x, mm	W_y, mm	V_x, mm	V_y, mm
Printed antenna	3.8	2400	32	30	39	28	23	18
Waveguide antenna ∅32 [15]	3.8	700	32	40	39	40	23	20

measurement of the brightness temperature for specific antennas. The relative power dissipated in a volume V can be calculated as follows:

$$L(V) = \frac{\int_V \frac{\sigma(r)}{2}\overline{E}(r)^2 dV}{\int_\infty \frac{\sigma(r)}{2}\overline{E}(r)^2 dV}. \quad (2)$$

Figure 4 shows the results of calculation of the volume for which the percentage of the total dissipated power of the antenna is 85%. In Fig. 4, W_z is the depth of measurement of the brightness temperature; W_x and W_y are the lateral dimensions of the area under study. The resolution is an important parameter of the antenna. By analogy with the theory of optical systems, the antenna resolution V_x along the X axis is defined here as the minimum distance between two single heat sources, at which these sources are distinguishable. The antenna resolution V_y along the Y axis is defined similarly. Two sources are considered distinguishable if the temperature between them is at least 20% below the maximum values.

The calculated parameters of the printed antenna and a waveguide antenna with a diameter of 32 mm used in a commercially available radiometer are compared in Table 2 [15] (F_0 is the central frequency, ΔF is the frequency bandwidth, and D is the antenna diameter).

The designed antenna has a significantly broader operating frequency band compared to currently used antennas (2400 MHz instead of 700 MHz). In this respect, it is comparable to the ultra-wideband spiral antenna described in [16]. However, it is rather difficult to build an IR temperature sensor into a spiral antenna. As for the measurement depth, the suggested antenna is slightly inferior to the waveguide antenna (30 vs. 40 mm). The cause is that the thickness of the dielectric substrate of the printed emitter is much smaller than that of the waveguide antenna. However, for many practical applications of a small-sized ultra-wideband antenna this is not critical.

Conclusions

The suggested printed ring-shaped antenna with a built-in IR temperature sensor is distinguished by its simplicity of design, small size, low height, and wider operating bandwidth. The antenna is manufactured using printed circuit board technology. Its expected cost is low. The antenna is intended for use as a part of a multichannel multifrequency radiometer. It is planned further to manufacture a prototype of the antenna, verify experimentally its characteristics, and conduct medical tests of the antenna when used as a part of a medical multichannel diagnostic system.

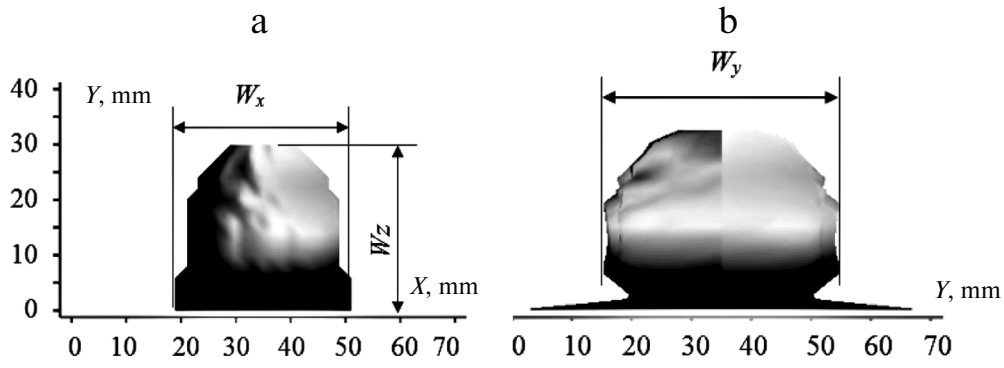

Fig. 4. Volume under study of brightness temperature measurement at the 85% level in the XZ (a) and YZ (b) planes.

This work was financially supported by the Russian Science Foundation (project No. 19-19-00349, April 24, 2019).

REFERENCES

1. Vesnin, S. G., Turnbull, A. K., Dixon, M. and Goryanin, I., "Modern microwave thermometry for breast cancer," J. Molec. Imag. Dynam., **7**, No. 2, 136 (2017).
2. Goryanin, I., Karbainov, S., Shevelev, O., Tarakanov, A., Redpath, K., Vesnin, S., and Ivanov, Y., "Passive microwave radiometry in biomedical studies," Drug Discovery Today, **25**, 757-763 (2020).
3. Drakopoulou, M., Moldovan, C., Toutouzas, K., and Tousoulis, D., "The role of microwave radiometry in carotid artery disease. Diagnostic and clinical prospective," Curr. Opin. Pharmacol., **39**, 99-104 (2018).
4. Cheboksarov, D. V., Butrov, A. V., Shevelev, O. A., Amcheslavsky, V. G., Pulina, N. N., Buntina, M. A., and Sokolov, I. M., "Diagnostic opportunities of noninvasive brain thermomonitoring," Anesteziol. Animatol., **60**, No. 1, 66-69 (2015).
5. Gudkov, A. G., Leushin, V. Yu., Vesnin, S. G., Sidorov, I. A., Sedankin, M. K., Solov'ev, Yu. V., Agasieva, S. V., Chizhikov, S. V., Gorbachev, D. A., and Vidyakin, S. I., "Studies of a microwave radiometer based on integrated circuits," Biomed. Eng., **53**, No. 6, 413-416 (2020).
6. Vesnin, S., Sedankin, M., Ovchinnikov, L., Leushin V., Skuratov, V., Nelin, I., and Konovalova, A., "Research of a microwave radiometer for monitoring of internal temperature of biological tissues," East.-Eur. J. Enterp. Technol., **4**, No. 5, 6-15 (2019).
7. Sedankin, M. K., Gudkov, A. G., Leushin, V. Yu., Vesnin, S. G., Sidorov, I. A., Chupina, D. N., Agasieva, S. V., Skuratov, V. A., and Chizhikov, S. V., "Microwave radiometry of the pelvic organs," Biomed. Eng., **53**, No. 4, 288-292 (2019).
8. Gudkov, A. G., Leushin, V. Yu., Sidorov, I. A., Vesnin, S. G., Porokhov, I. O., Sedankin, M. K., Agasieva, S. V., Chizhikov, S. V., Gorlacheva, E. N., Lazarenko, M. I., and Shashurin, V. D., "Use of multichannel microwave radiometry for functional diagnostics of the brain," Biomed. Eng., **53**, No. 2, 108-111 (2019).
9. Gudkov, A. G., Sedankin, M. K., Leushin, V. Yu., Vesnin, S. G., Sidorov, I. A., Agasieva, S. V., Ovchinnikov, L. M., and Vetrova, N. A., "Antenna applicators for medical microwave radiometers," Biomed. Eng., **52**, No. 4, 235-238 (2018).
10. Sedankin, M. K., Chupina, D. N., Nelin, I. V., and Skuratov, V. A., "Development of patch textile antenna for medical robots," in: 2018 Int. Conf. Actual Problems of Electron Devices Engineering (APEDE), IEEE (2018), pp. 413-420.
11. http://www.radiometry.ru/rtm-01-res/description/.
12. Lauk-Dubitskiy, S. E., Pushkarev, A. V., and Korovin, I. A., "Porcine heart valve, aorta and trachea cryopreservation and thawing using polydimethylsiloxane," Cryobiology, **93**, 91-101 (2020).
13. Burkov, I. A., Pushkarev, A. V., Shakurov, A. V., Tsiganov, D. I., and Zherdev, A. A., "Numerical simulation of multiprobe cryoablation synergy using heat source boundary," Int. J. Heat Mass Transf., **147**, Article No. 118946 (2020).
14. Zakirov, A., Belousov, S., Valuev, I., Levchenko, V., Perepelkina, A., and Zempo, Y., "Using memory-efficient algorithm for large-scale time-domain modeling of surface plasmon polaritons propagation in organic light emitting diodes," J. Phys.: Conf. Ser., No. 905, 012-030 (2017).
15. Sedankin, M. K., Leushin, V. Yu., Gudkov, A. G., Vesnin, S. G., Khromov, D. A., Porokhov, I. O., Sidorov, I. A., Agasieva, S. V., and Gorlacheva, E. N., "Modeling of thermal radiation by the kidney in the microwave range," Biomed. Eng., **53**, No. 1, 60-65 (2019).
16. Rodrigues, D. B., Maccarini, P. F., Salahi, S., Oliveira, T. R., Pereira, P. J., Limro-Vieira, P., and Stauffer, P. R., "Design and optimization of an ultra wideband and compact microwave antenna for radiometric monitoring of brain temperature," IEEE Trans. Biomed. Eng., **61**, No. 7, 2154-2160 (2014).